Journal Pre-proof

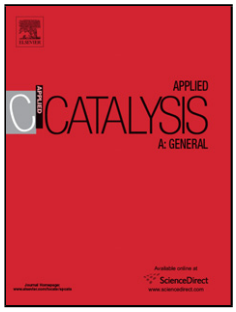

Aldol condensation of acetic acid and formaldehyde to acrylic acid over a hydrothermally treated silica gel-supported B-P-V-W oxide

R. Nebesnyi, Z. Pikh, V. Sydorchuk, S. Khalameida, I. Kubitska, O. Khyzhun, A. Pavliuk, T. Voronchak

PII: S0926-860X(20)30065-X

DOI: https://doi.org/10.1016/j.apcata.2020.117472

Reference: APCATA 117472

To appear in: *Applied Catalysis A, General*

Received Date: 26 November 2019

Revised Date: 11 February 2020

Accepted Date: 17 February 2020

Please cite this article as: Nebesnyi R, Pikh Z, Sydorchuk V, Khalameida S, Kubitska I, Khyzhun O, Pavliuk A, Voronchak T, Aldol condensation of acetic acid and formaldehyde to acrylic acid over a hydrothermally treated silica gel-supported B-P-V-W oxide, *Applied Catalysis A, General* (2020), doi: https://doi.org/10.1016/j.apcata.2020.117472

Aldol condensation of acetic acid and formaldehyde to acrylic acid over a hydrothermally treated silica gel-supported B-P-V-W oxide

R. Nebesnyi[a], Z. Pikh[a], V. Sydorchuk[b], S. Khalameida[b*], I. Kubitska[a], O. Khyzhun[c], A. Pavliuk[a], T. Voronchak[d]

[a] *Technology of Organic Products Department, Lviv Polytechnic National University, 12 S. Bandera Str., 79013, Lviv, Ukraine*

[b] *Institute for Sorption and Problems of Endoecology, NAS of Ukraine, 13 Naumov St., 03164 Kyiv, Ukraine; *E-mail: svkhal@ukr.net*

[c] *I.M. Frantsevych Institute for Problems of Materials Science, NAS of Ukraine, 3 Krzhyzhanovsky St., 03680, Kyiv, Ukraine*

[d] *Market Central Laboratory, Nestle Ukraine LLC, Malekhiv, 2a Kyivska str., 80383, Lviv region, Ukraine*

Graphical abstract

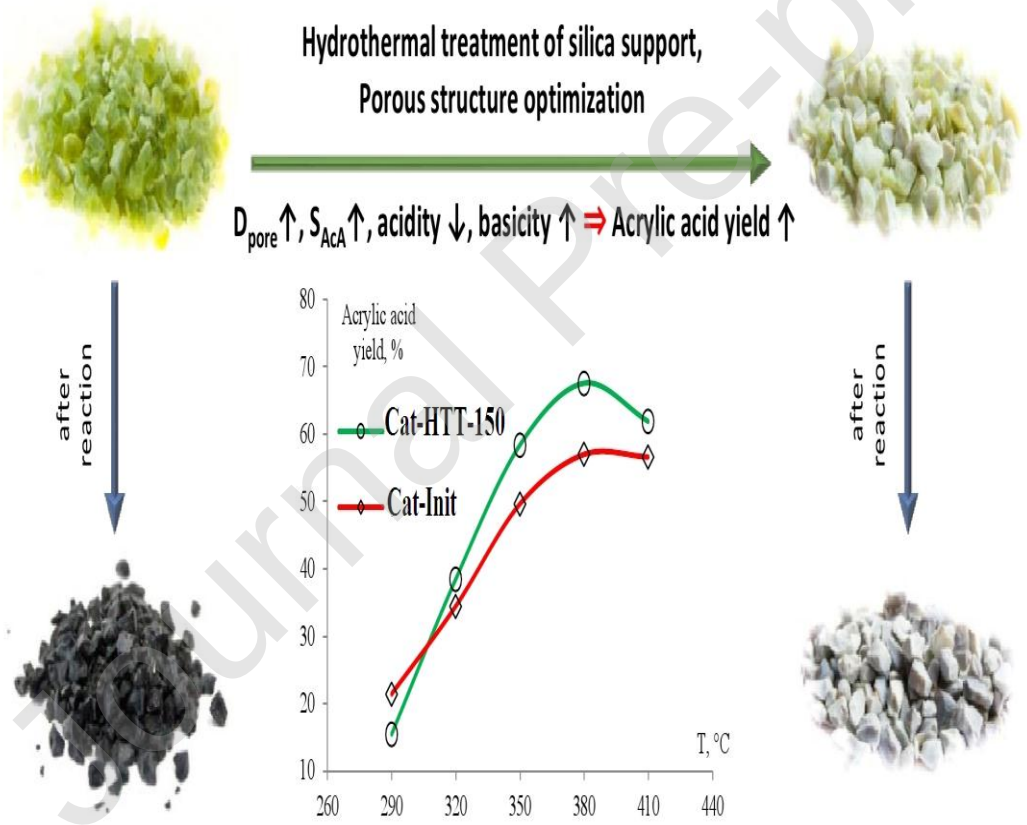

Higlights

- B-P-W-V oxide catalysts based on hydrothermally treated silica support were developed and studied in aldol condensation of acetic acid with formaldehyde to acrylic acid reaction.

- Hydrothermal treatment of silica support results in formation of catalyst porous structure more accessible for reagents molecules.

- Supported catalysts based on hydrothermally treated silica has lesser content of acid sites and more ability to acetic acid sorption.

- Hydrothermal treatment of silica support at 150°C is optimal for preparation of catalyst possessing the best catalytic performances.

- The best catalyst allows to achieve acrylic acid yield up to 67.6% which is 10% higher than for catalyst based on untreated support.

Abstract:

Supported on silica B-P-V-W-O_x catalysts of the aldol condensation process, subjected to hydrothermal treatment (HTT), were synthesized and characterized. It was found that HTT of silica has a significant effect on catalyst texture, namely specific surface area, pore size. These properties affect the distribution of the active phase on the support surface. It was suggested that this is the reason of change in acid-base characteristics of the catalysts. It was observed that HTT at 100-150°C leads to increase in surface, available for the reagents, ability to sorb acetic acid, decrease of acidity, improving catalytic activity and selectivity. It had been demonstrated that HTT allows to increase acrylic acid yield up to 67.6% which is 10% higher compared to that for catalyst supported on initial silica. The HTT of silica support before the active phase deposition is suggested as a cheap and efficient way to improve catalytic performance of B-P-V-W-O_x/SiO_2 catalysts.

Keywords – acrylic acid; aldol condensation; solid catalysts; porous structure; hydrothermal treatment.

1. Introduction

Acrylic acid (AA) is a large-scale chemical, world production capacity of which exceeds 5 million tons annually. Acrylic acid and its derivatives are used to produce high-quality paints and varnishes, organic glass, concrete modifiers and as intermediate substances for fine organic synthesis. Today, main industrial AA production method is two-stage oxidation of propylene *via* intermediate stage of acrolein formation [1,2]. This method proved itself to be good in terms of economic efficiency and equipment design simplicity. However, petroleum-based origin of

propylene and volatility of world oil market cause need of development of alternative methods of AA and its derivatives production. So, the development of alternative methods of acrylic acid synthesis, in particular from renewable raw materials, became a new trend. Such alternative method of AA synthesis can be one of the following: 1) AA synthesis based on biomass using

* Corresponding author: Svitlana Khalameida. Tel. +38 044 452-93-28; E-mail:svkhal@ukr.net

enzymes; 2) AA synthesis based on glycerol as a by-product of biodiesel production; 3) AA synthesis by aldol condensation of acetic acid (AcA) with formaldehyde (FA) [2,3]. Production of AA from renewable raw materials is carried out by fermentation of biomass to 2-hydroxypropanoic or 3-hydroxypropanoic acid with further dehydration to AA. The principal weakness of this approach is considerable duration of the process [4-6] and consequently low productivity of reaction equipment. There are numerous publications dedicated to glycerol oxy-dehydration into acrolein and acrylic acid [4]. One-pot glycerol oxy-dehydration to AA over multifunctional catalysts was also reported [5], but the highest AA yield does not exceed 50 – 75 % at comparatively low process selectivity.

AA production by aldol condensation of AcA with FA (*via* the scheme: biomass (natural gas, coal) – syngas – methanol – acetic acid and formaldehyde – acrylic acid) also can be considered as a promising approach. Acetic acid is produced mostly *via* the Monsanto process (catalytic carbonylation of methanol) and formaldehyde is produced by oxidation of methanol. Both acetic acid and formaldehyde are relatively cheap and widely available chemicals. However, industrial-scale AA production by aldol condensation has not been arranged so far, because of insufficient performance of known catalysts of the process. Besides low efficiency of known catalysts of aldol condensation of unsaturated carboxylic acids with formaldehyde, their another disadvantage is short working time because of coke deposition on their surface [2,7]. That is why development of new highly efficient catalysts for AA production by aldol condensation of AcA with FA without aforementioned disadvantages is still very urgent.

A lot of publications are devoted to AA synthesis on V-P-O catalysts. Early studies describe the use of vanadium and mixed vanadium-titanium phosphates [8,9]. The used catalysts possessed insufficient specific surface area, undeveloped porous structure and required granulation. Therefore, in order to increase their productivity, the supported catalysts (predominantly based on silica as a support) were tested in this process [10-12]. The authors found that the balance between acid and base sites and the ratio of V^{4+} and V^{5+} had significant influence on catalytic performance and this ratio is dependent on V and P content [11]. The authors also noticed that calcination temperature effected on catalysts texture, and both textural properties and ratio of V^{4+}/V^{5+} of V-P-O catalyst could be considered to be the main factors favoring the catalytic performance increase [10]. However, despite the high specific surface area and developed porous structure, these catalysts did not show good catalytic performance. The highest yield of AA was only 21.9% with a selectivity respect to AA 97.8%.

Better results were obtained with V-P-O catalyst deposited on supports with regular porosity, namely SBA-15 and HZSM-5. The acrylic acid selectivity was 90.8 – 70.2% at the formaldehyde conversion of 14.3 – 68.7% [13]. It was found that the catalytic performance, among other factors, depends on acid and base properties of the catalyst, and the acid and base sites number were significantly affected by the support type and P/V atomic ratio. The SBA-15-supported V-P-O catalysts with high number of both acid and base sites exhibited high catalytic activity in the aldol condensation of AcA with formaldehyde to AA. On the other hand, V-P-O/SBA-15 catalyst possesses the highest specific surface area among the tested catalysts and the authors noticed that the correlation between catalyst structure and its activity is worth of further study. The later paper [14] describes the effect of Cs, Ce, and Nd cations on the efficiency of V-P-O/SiO_2 catalysts. The addition of the metallic cations in the catalysts increased their basicity, while their acidity increased at a lower ratio of metallic cation to vanadium. It was also noted that the presence of the metallic cations also increased the V^{5+}/V^{4+} ratio. Maximum AA yield on

Ce-V-P-O/SiO_2 catalysts was 73.9%. It should be noted that in papers [13,14] the acetic acid/formaldehyde mole ratio was 3:1.

The particularity of all above-mentioned papers [10-14] is that the catalysts structure was changed as a result of change in qualitative and quantitative composition of the catalysts or the support type and, as a result, a lot of characteristics of the catalysts' surface were changed (specific surface area, pore size, acid and base properties, V^{5+}/V^{4+} ratios). Thus, it is quite difficult to separate one factor and its impact on catalytic performance from another.

In our previous studies, the catalysts of the following qualitative composition: B–P–V–W–O_x/SiO_2 was described. These catalysts are rather efficient in gas-phase aldol condensation of AcA with FA to AA. It was found out that the optimal atomic ratio of the catalyst components B:P:V:W is 3:1:0.18:0.12 and this type of catalysts is effective even at equimolar ratio of AcA and FA in the reaction mixture [3, 15-18]. The aim of the present paper is to determine the effect of the catalyst porous structure on its catalytic performance in aldol condensation of AA with formaldehyde at constant qualitative and quantitative composition of the catalysts. It is well known that porous structure of solid catalysts has a significant effect on their catalytic properties. To modify structure of porous materials such method as hydrothermal treatment is widely used. Hydrothermal treatment (HTT) is effective procedure for regulation of porous, crystal and surface structure of adsorbents, catalysts and their supports [19-21]. Particularly, HTT of different kinds of silica has been extensively studied [19-26]. This method allows to vary the parameters of silica gel porous structure in a very wide range. The elevation of HTT temperature results in monotonic and significant reduction in specific surface area and increase of pore size at constant pore volume [20,23,24]. Besides, increase in mechanical strength of silica gel granules takes place up to the treatment temperature about 250°C [24, 27-29].

In present work it was important to ascertain the effect of HTT of the silica support for B–P–V–W–O_x catalyst on its efficiency in the process of AA production by aldol condensation of AcA with FA. It was also important to find out exactly, what values of the catalyst support characteristics, achieved by means of HTT, ensure catalytic efficiency of the catalyst in aldol condensation of AcA with FA to form AA.

2. Experimental

2.1. Materials

Silica gel with a specific surface area 365 m^2/g (China) was used as a catalyst support. AR grade chemicals H_3BO_3, $(NH_4)_2HPO_4$, $H_7(P(W_2O_7)_6)\cdot H_2O$ and NH_4VO_3 (Sigma-Aldrich) were used for the catalyst preparation. AR grade AcA and FA (Sigma-Aldrich) were used for the catalyst testing in chemical reaction. 37% formalin was used as a source of FA, and the formalin was obtained from paraformaldehyde (Sigma-Aldrich).

2.2. Catalyst preparation

To regulate the porous structure of the support, silica gel was subjected to HTT in the temperature range 100-250°C for 3 h. The treatment was carried out in the vapor-phase [20, 22] using laboratory steel autoclave of 45 mL volume. The weight of silica (10 g) was placed in a PTFE vessel and water (5-10 mL depending on temperature of HTT) was poured on the bottom of the autoclave. After HTT, the support was dried at 100°C for 5 h.

The active phase of the catalyst was deposited on initial and hydrothermally treated supports by impregnation. Aqueous solutions of H_3BO_3, $(NH_4)_2HPO_4$, $H_7(P(W_2O_7)_6)$ and NH_4VO_3 taken in amounts to ensure atomic ratio of the catalyst components B:P:V:W to be 3:1:0.18:0.12 in finished catalyst, were used for the catalyst preparation. After the impregnation the catalyst precursor was dried at 150°C for 8 h and then calcined in air at 400°C for 6 h. The

finished catalysts contain about 20 %w/w of active phase. The prepared supported catalysts based on initial and treated silica are hereinafter named as Cat-Init and Cat-HTT-t (where t – temperature of silica HTT), respectively. Bulk catalyst (without support) was prepared under the same conditions.

2.3. Catalyst characterization

The porous structure of the prepared supports and catalysts was studied using the adsorption-structural methods. Nitrogen isotherms of adsorption-desorption were obtained using an automatic gas adsorption analyzer ASAP 2405N (by Micromeritics Instrument Corp.) after outgassing the samples at 150°C for 2 h. The specific surface area *S*, volume of mesopores V_{me} and volume of micropores were calculated from these isotherms using the BET, BJH and t-method, respectively. The total pore volume V_{Σ} was determined by means of impregnation of the samples granules after their drying at 150°C with liquid water (so-called incipient wetness method) [30]. The curves of pore size distribution (PSD) were plotted using the desorption branches of isotherms. Besides, the isotherms for one of the reagents, namely acetic acid, were obtained at 20°C from vapour phase to relative pressure p/p_0=0.5 using the adsorption setup with the McBan-Bakr spiral quartz balances [30]. Before measurements, the samples were degassed at residual pressure 10^{-3} Pa and 150°C for 2 h. This data has been used for two purposes: 1) for calculation of specific surface area accessible for acetic acid S_{AcA}; 2) for estimation of basic properties for the supported catalysts.

The crystal structure of the catalysts was studied by means of X-ray powder diffraction (XRD) using Philips PW 1830 diffractometer with CuKα-radiation. The FTIR spectra in the range 4000 – 400 cm^{-1} were registered using the "Spectrum-One" spectrometer (by Perkin-Elmer). The ratio of sample and KBr powder was 1:20. KBr was dried at 600°C for 2h before the measurements.

The selected samples have been tested with X-ray photoelectron spectroscopy (XPS) to measure the binding energies (BEs) of the core-level electrons as well as the energy distribution of the valence electronic states (XPS valence-band spectra). The XPS spectra were acquired with the UHV-Analysis-System. The system was designed and assembled by SPECS Surface Nano Analysis Company (Berlin, Germany).

The curves of DTA-TG for spent catalysts (tested for 8 h) were registered in air using the Derivatograph-C apparatus (F.Paulik, J.Paulik, L.Erdey system) from 20 to 1000°C at a heating rate 10 °/min. The initial mass of the sample was 200 mg.

Surface acidity of supported catalysts was determined using temperature-programmed desorption of ammonia [30]. The sample was placed in a glass reactor and heated to 410°C in a flow of helium. This temperature of pretreatment is selected since the catalytic tests were carried out at a temperature ≤ 410°C. Then the sample cooled to 20 ºC and saturated with ammonia. Next heating of the sample was carried out at a rate 17 °/min. The thermodesorption of ammonia was carried out in the temperature range 20-650°C. The amount of desorbed ammonia was determined by titration with hydrochloric acid at the outlet from the reactor.

2.4. Catalysts performance study

Catalytic performance of the catalysts in aldol condensation of AcA with FA to AA was studied in a fixed bed flow reactor. The reactor was made of stainless-steel tube (250 mm long, 10 mm I.D.) mounted vertically and equipped with electric heating. Amount of catalyst with granule size of 1.5-3 mm was 3.5 g. Before being used the catalysts were dried at 150°C for 2 h.

A reaction was carried out under atmospheric pressure from 290 to 410°C and space time 8 s. The reactants molar ratio AcA:FA = 1:1. The reaction products composition was determined by gas chromatography (instrument HP 6890). A capillary chromatographic column Restek with 30 m length and Srabilwax as stationary phase is used. The main products were acrylic acid,

acetone and carbon dioxide. The molar ratios of CO_2 to acetone were close to 1, indicating that both CO_2 and acetone are formed in the same reaction of acetic acid ketonization. So the catalytic performance was evaluated by acrylic acid selectivity and yield as well as by acetic acid conversion.

The yield and selectivity were calculated based on the amount of acetic acid fed into the reactor. The acrylic acid yield (Y_{AA}) is defined as 100 moles of acrylic acid / moles of acetic acid fed in. The acrylic acid selectivity (S_{AA}) is defined as 100 moles of acrylic acid / moles of acetic acid consumption. The acetic acid conversion (X_{AcA}) is defined as 100 moles of acetic acid consumption / moles of acetic acid fed in. Carbon balance (>90%) was achieved under reaction conditions which is acceptable for such reactions [5].

3. Results and Discussion

3.1. Catalyst characteristics

3.1.1. Porous structure

It was very important to find out the effect of HTT on the catalyst performance, so first of all the porous structure of treated supports and supported catalysts were characterized. The obtained results for silica gel HTT, based on nitrogen adsorption-desorption isotherms (Fig. S1) are quite consistent with those described in literature [8, 9, 11, 12]. The PSD curves calculated from desorption branches of isotherms (insets to Fig. S1) show that the maximum is shifted towards higher values of pore diameter when temperature of HTT increases.

All samples are mesoporous and the values of V_Σ and V_{me} are almost identical (compare columns 4 and 5 of Table 1) and there are no micropores. Thus, we have the uniformly mesoporous supports, specific surface area of which monotonically decreases while the pore size monotonically increases, and the pore volume remains almost constant with HTT temperature elevation (Table 1). PSD curves obtained for silica gel, subjected to treatment at 200-250°C, are diffused (Fig. S1). Consequently, these supports have a less uniform pore structure than those modified at 100-175°C.

Table 1. Porous structure parameters of silica supports

N	Sample	S_{N2} (m^2/g)	V_Σ (cm^3/g)	V_{me} (cm^3/g)	d (nm)
1	2	3	4	5	6
1	Initial silica	365	1.05	1.04	7.9
2	HTT at 100°C	350	1.05	1.07	7.9
3	HTT at 125°C	316	1.04	1.04	8.7
4	HTT at 150°C	275	1.04	1.02	9.7
5	HTT at 175°C	201	0.99	1.00	13.6
6	HTT at 200°C	141	0.92	0.91	17.9
7	HTT at 225°C	119	0.96	0.97	25.0
8	HTT at 250°C	102	0.98	0.96	31.5

The deposition of active phase onto all supports are accompanied by decrease both of specific surface area and pore volume V_Σ but values of V_Σ are almost the same for all supported catalysts (Fig. S2, Table 2). This is associated with partial filling of pores by deposited phase. Nevertheless, the value of specific surface area of supported catalysts calculated by acetic acid sorption S_{AcA} is lower than S_{N2} for the catalysts prepared from silica gel treated at temperature <150°C. Besides, S_{AcA} has maximum value for the catalyst based on silica treated at 150°C (Cat-HTT-150). This is evidence that part of the surface is inaccessible for larger molecules of acetic acid – its kinetic diameter is 0.44 nm against 0.36 nm for N_2. At the same time, both values of

specific surface area practically coincide for catalysts prepared using silica treated at 150°C and higher temperature. In other words, elevation of HTT temperature is accompanied by increase in pore size both of support and corresponding catalyst and shift of PSD curves towards higher *d* values. As a result, accessibility of pores for AcA molecules and therefore S_{AcA} value also increase. After HTT at 150ºC, pores diameter from maximum on PSD curves reaches value (9.7 nm for support and 12.3 nm for catalyst) that ensures complete accessibility of the pore surface for AcA molecules. At higher HTT temperatures, the pore diameter continues to increase, and the values of S_{AcA} and S_{N2} monotonously decrease. This is possible if the supported catalysts contain bottle-shaped pores, so-called "ink-bottle effect" [31,32]. Such effect can be eliminated as a result of hydrothermal or mechanochemical treatment by increasing the size of the entrances to the pores, as was observed for silica gel and zirconium phosphate [19,33]. Therefore, the accessibility of pores for adsorbate molecules, used for specific surface area measurements, as well as reagents in catalytic processes increases [19,32,33]. The pore size of the catalysts also increases compared to corresponding supports (compare insets to Fig. S1 and Fig. S2).

Table 2. Parameters of porous structure of supported catalysts

N	Sample	Fresh catalyst				Spent catalyst		
		S_{N2} (m^2/g)	S_{AcA} (m^2/g)	V_{Σ} (cm^3/g)	*d* (nm)	S_{N2} (m^2/g)	V_{Σ} (cm^3/g)	*d* (nm)
1	2	3	4	5	6	7	8	9
1	Cat-Init	238	178	0.74	9.7	238	0.69	8.0
2	Cat-HTT-100	245	180	0.75	9.7	251	0.72	8.7
3	Cat-HTT-125	232	190	0.74	11.1	241	0.75	9.6
4	Cat-HTT-150	193	197	0.72	12.6	199	0.74	12.3
5	Cat-HTT-175	130	128	0.65	14.8	138	0.64	14.8
6	Cat-HTT-200	107	110	0.73	17.8	110	0.74	17.8
7	Cat-HTT-225	84	n.d.	0.70	24.4	79	0.69	23.4
8	Cat-HTT-250	62	n.d.	0.72	31.8	55	0.72	32.0

The prepared supported catalysts have thermostable porous structure in reaction mixture (Table 2): its parameters practically did not change in the temperature range, in which the catalytic tests were performed (subsection 3.2). Only the spent catalyst (after 8 hours of the reaction) based on initial silica and those ones after HTT at low-temperature (100-125°C) have less values of total pore volume and size of mesopores compared to those for corresponding fresh catalysts. This may be due to coking process, which is obviously possible in narrow pores (up to 10-11 nm) but is less likely in pores of larger size. Indeed, the granules of catalyst, prepared from initial silica (Cat-Init), become almost black after the catalytic test (Fig. 1). As higher the HTT temperature for silica (or as wider the pores both of the support and corresponding catalyst) is, the lighter color of the spent catalyst granules is (Fig. 1). So, the catalysts, which are based on silica hydrothermally treated at 150°C and above, might have longer catalyst life.

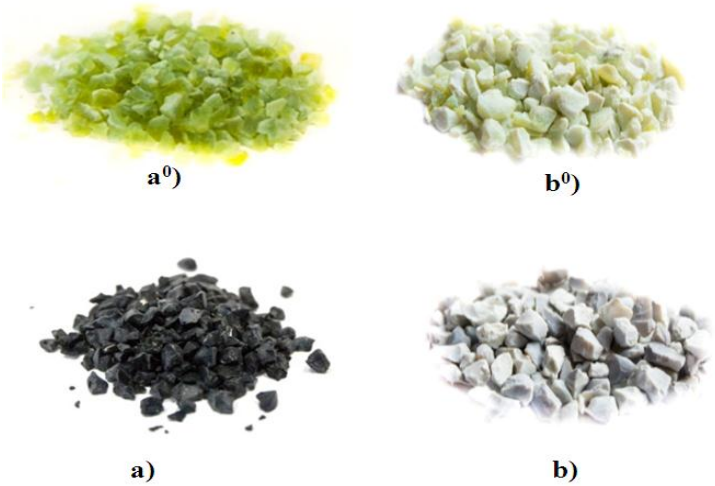

Fig. 1. Granules of B–P–V–W–O_x/SiO_2 catalysts: a^0–Cat-Init (fresh catalyst), *a*–Cat-Init (spent catalyst), b^0–Cat-HTT-150 (fresh catalyst) and *b*–Cat-HTT-150 (spent catalyst)

Besides, the results of DTA-TG analysis confirm the formation of carbonaceous deposits on the catalysts surface as shown in other studies [34-36]. The mass loss within 300-500°C, which corresponds to exoeffect at 400-450°C, indicates this. The mass loss and exoeffect are attributed to combustion of carbon deposits (coke) in the catalyst's pores. The coking degree decreases with elevation of support HTT temperature, which is associated with increase of pore size. Minimal mass loss value of 0.7%w/w was registered for spent catalyst based on silica gel hydrothermally treated at 250°C (Cat-HTT-250) while maximal value, which is about 5%w/w, was obtained for spent catalyst Cat-Init. For spent catalyst based on treated at 150°C mass loss is about 1%w/w. The examples of such DTA-TG curves are present on Fig. S3.

3.1.2. Crystal and surface structure

The crystal structure of bulk and supported catalysts was studied by means of XRD and FTIR spectroscopy. The obtained diffractograms are shown in Fig. 2. It can be seen, that only reflexes attributed to boron oxide B_2O_3 are present in diffractograms for bulk catalysts (unsupported B–P–V–W–O_x): there are peaks at 2Θ = 14.64; 24.60; 28.06 and several low-intensity peaks around 2Θ =39-41° (curves *a*, *b*) [37]. The position and intensity of main reflexes is somewhat different as a result of active phase deposition. Thus, reflexes at 2Θ = 14.64 and 24.60° is superimposed on the halo (curves *c*, *d*), which is typical for amorphous silica. The diffraction patterns are not changed after catalysis (compare curves *a*, *b* and *c*, *d* in Fig. 2). The calculation of crystallite size *D* for B_2O_3 using Sherrer's equation allows to estimate the degree of dispersion of the deposited phase. The most intense reflex 2Θ = 24.60° was used for this purpose. The comparison of the *D* values for bulk and supported samples indicates that B_2O_3 crystallites have a smaller size for the latter catalysts. Thus, for the bulk sample *D* is 37.2 nm, for the catalyst supported on initial silica gel – 29.6 nm, and for the catalysts supported on silica gel after HTT at 150-250 °C – 23-25 nm. The latter indicates the dispersion of the active phase on the surface of the support.

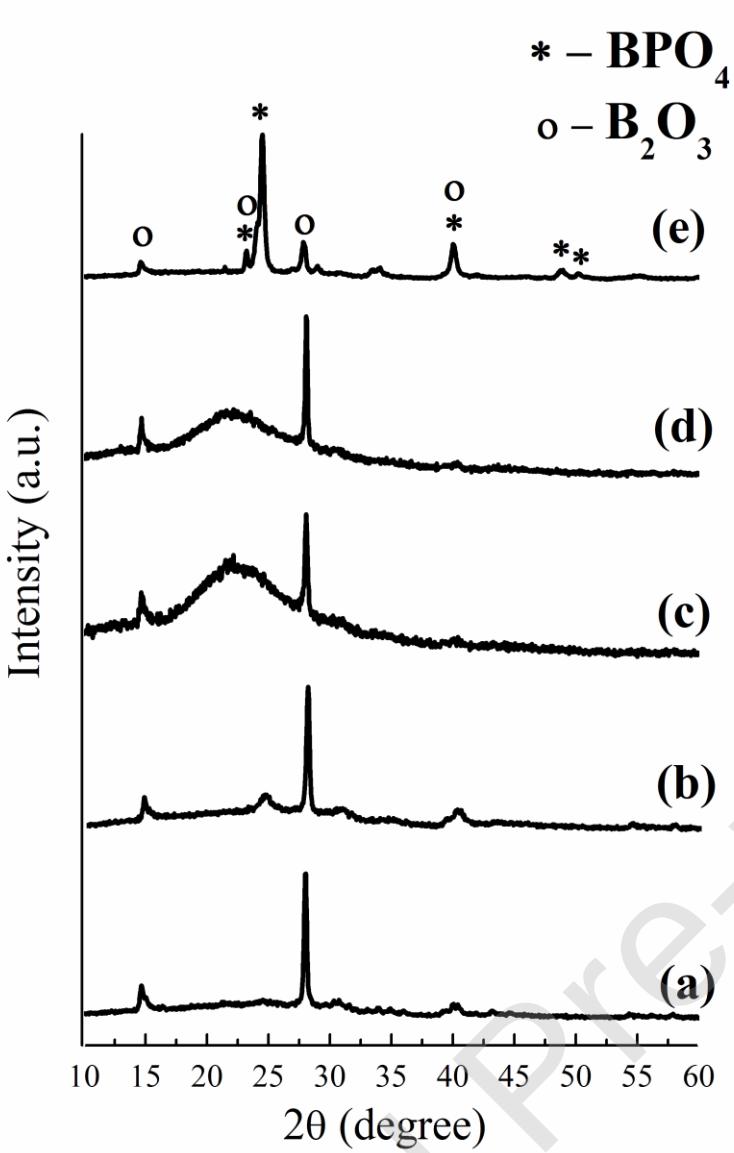

Fig. 2. X-Ray difractograms for bulk catalyst before (a), after catalysis (b) and catalyst Cat-HTT-150 before (c), after catalysis (d) and bulk catalyst calcined at 600 ^{o}C (e).

Phosphorus oxide, obviously, is a part of amorphous or X-ray amorphous phases. For example, it can form amorphous boron phosphate BPO_4 with part of boron oxide. Indeed, bulk catalysts contain a mixture of crystalline B_2O_3 and BPO_4 after calcinations at 600^{o}C when amorphous component is crystallized (Fig. 2, curve *e*). Particularly, the peaks at 2Θ = 23.21, 24.52, 40.02, 48.90, 50.20^{o} are attributed to BPO_4 (JCPDS N 00–034–0132) [37-40]. The characterization of bulk catalyst was performed because of small amount of active phase in the catalyst, so the changes of reflexes for bulk catalyst is easier to notice.

Analysis of FTIR spectra (despite substantial overlapping of absorption bands - a.b. - attributed to support and active phase) allowed additionally to determine structure of catalysts. In general, FTIR spectra confirm the XRD data. The most intensive a.b. in the FTIR spectra for bulk catalysts, which are recorded in the absorbance mode, are also attributed to B_2O_3 (Fig. S4): 3208, 1459, 1379, 1195, 885, 800, 651, 549 cm^{-1} [37,41]. Besides, a.b. centered at 1090-1120, 930-950, 610-640 and 550-560 cm^{-1} are revealed in spectra of bulk catalysts. They are assigned to BPO_4 [37-40].

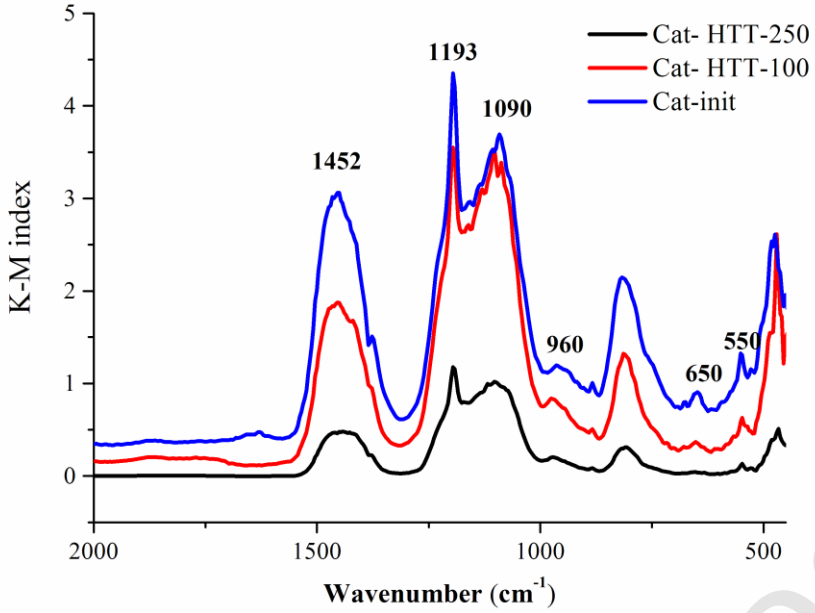

Fig. 3. FTIR spectra of the B–P–V–W–O_x catalyst supported on initial and treated silicas

However, these bands cannot be clearly detected for supported catalysts due to the strong overlapping with bands related to siliceous support (Fig. 3). Intensive a.b. around 3208 cm^{-1} is revealed in spectra for bulk and supported catalysts (Fig. 4). This band is attributed to stretching vibrations of surface OH-groups both for boron oxide and phosphate [39,40,42]. As can be seen in Fig. 4, the reduction in the intensity of a.b. at 3208 cm^{-1} is observed as a result of the support HTT temperature elevation.

Also, a.b. as shoulder at 3650-3700 cm^{-1} is present in all spectra. It is obviously assigned to stretching vibrations of surface SiOH-groups of silica support [19,25,26]. Low intensity of this a.b. compared to that for the pure silica (Fig. 4) is observed. At the same time, its intensity is reduced with elevation of the support HTT temperature. The latter can be explained by a specific surface area decreasing (Table 1, column 3), as well as by denser coating of the support surface with the deposited phase. Indeed, constant content of deposited phase (20 %w/w) is distributed onto a smaller surface and covers it more densely.

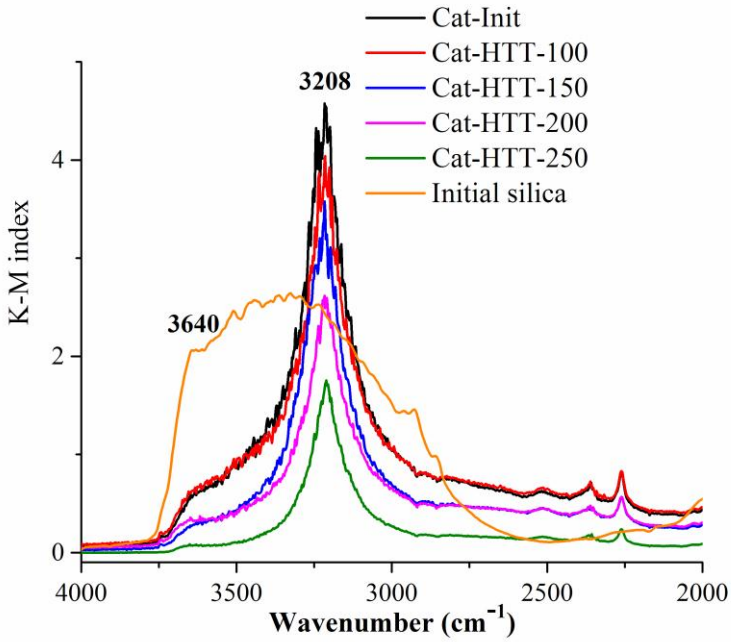

Fig. 4. Band of stretching vibrations of surface OH-groups in FTIR spectra for initial silica and B–P–V–W–O_x catalyst supported on initial silica and silica treated by HTT at various temperatures

Surface state of atoms was evaluated using XPS. Thus, survey XPS spectra of the fresh catalysts 1 and 4 from Table 2 as well as the bulk catalyst are presented in Fig. 5. XPS O1s, Si2P, P2p, B1s core-level spectra for these catalysts are presented on Figs. S5-S8. As can be seen, the positions and shape of peaks change a little as a result of deposition on silica. Their binding energies are as follows: 532.9, 103.4, 134.6-134.9 and 193.2 eV. First value is close to those for oxygen in B_2O_3 and SiO_2 – 533.5 and 532.3 eV [42, 43]. Other values obviously correspond to silicon in SiO_2, phosphorus in meta-phosphates, boron in B_2O_3 (and/or BPO_4), respectively [44]. It should be noted that binding energies of B1s for B_2O_3 and BPO_4 differ only by 0.3-0.5 eV [37]. XPS spectra associated with W is rather small by its intensity (its content is about 1.0 %w/w in the supported catalysts), but it is possible to determine binding energy of the most informative W $4f_{7/2}$ core-level spectra of this chemical element (36.6 eV). Comparison with literature data [44,45] indicates that tungsten is in the effective charge states +6 in studied catalysts. The presence of vanadium is very difficult to determine in the analysed layers even for the bulk sample and especially for the both supported samples under consideration due to its low content (about 1.5 %w/w in supported catalysts) and perhaps also due to the fact that it is mainly located in the subsurface layer (deeper than 3 nm). Nevertheless, a low-intensity diffuse peak with a maximum, which can be divided into two components centered about 516.4 and 517.4 eV, is visible (Fig. S5, inset). They can be attributed to V^{4+} 2p 3/2 and V^{5+} 2p 3/2, respectively [11]. However, it is not possible to establish the V^{4+}/V^{5+} ratio, as was done in [11]. Indeed, the catalysts are greenish, indicating the presence of V^{4+} (Fig. 3).

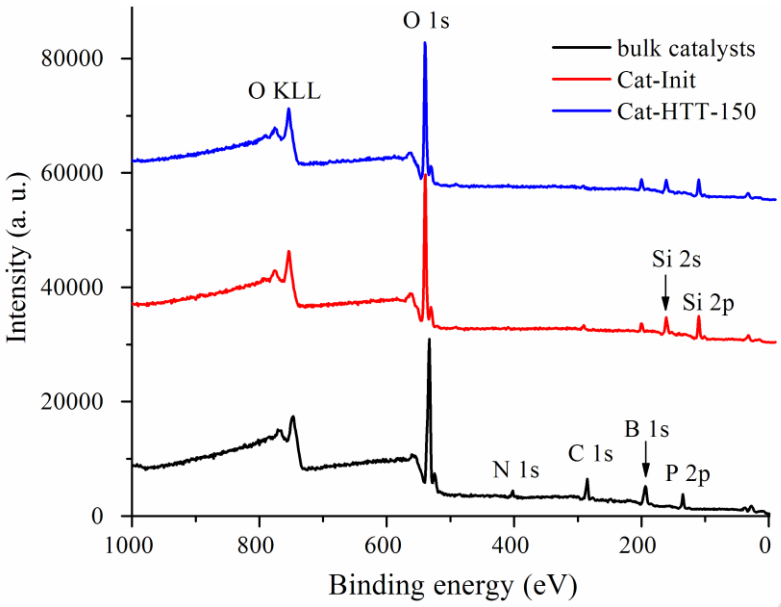

Fig. 5. Survey XPS spectra of the bulk, Cat-Init and Cat-HTT-150 catalysts.

Table 3 shows surface content of analyzed elements for bulk catalyst as well as for Cat-Init and Cat-HTT-150 catalysts, namely supported on initial and hydrothermally treated at 150°C silica gel. Two differences between these catalysts should be noted: /i/ decrease of phosphorus content in a row: bulk catalyst - Cat-Init – Cat-HTT-150; this may be the reason for the minimum concentration of acid sites for Cat-HTT-150 (see below, Table 4, column 5); /ii/ simultaneous decrease in silicon concentration and increase in boron concentration (two elements with the highest content) or increase in surface B/Si ratio from 0.73 to 1,28. The latter may indicate more complete covering the silica surface by deposited phase for Cat-HTT-150. The presence of nitrogen in bulk catalyst (Fig. 5, Table 2) can be associated with incomplete thermodestruction of ammonium salts that are used as reagents for the preparation of catalysts. Indeed, maximum positioned at 401.9 eV corresponds to nitrogen in oxidation state -3 [44]. The absence of this peak in the spectra obtained for supported catalysts can be explained by complete destruction of ammonium salts on silica surface.

Table 3. Elemental content (at. %) in the analysis surface layers of the bulk and supported catalysts.

Sample	O	Si	P	B	W	C	V	N
Bulk catalyst	45.9	-	7.3	27.1	0.9	15.3	0.4	3.1
Cat-Init	58.1	21.5	1.3	15.6	0.3	3.2	-	-
Cat-HTT-150	58.7	16.7	1.1	21.3	0.2	2.0	-	-

Therefore, based on the XRD and FTIR results, it can be assumed that the deposited layer consists of phases of boron oxide and phosphate in amorphous and crystalline states. The state of vanadium and tungsten in the catalyst structure cannot be determined using indicated techniques due to their low concentration (about 1.5 %w/w in supported catalysts). Perhaps they play the role of dopants like other metals for supported V-P-O catalysts of aldol condensation of AcA with FA, which regulate their acid-base properties [14].

The examples of TEM micrographs of catalyst Cat-HTT-150 are presented in Fig. 6. Particularly, image 6*a* demonstrates sufficiently uniform distribution of active phase on the structure of the support. At the same time, the histograms based on images 6b and 6c with higher resolution have maxima for particle size about 75-80 nm. Obviously, these are aggregates of crystallites with a size of about 23-25 nm, as was shown above by the Scherrer method.

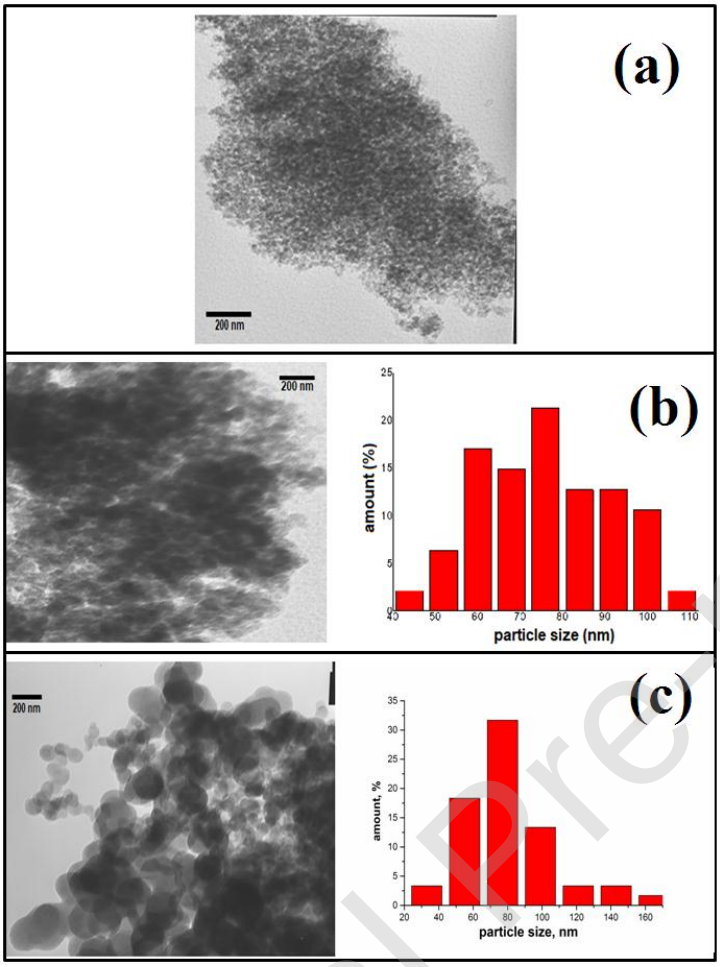

Fig. 6. TEM micrographs of supported catalyst Cat-HTT-150. The magnification was 56000 (a), 72000 (b) and 100000 (c)

3.1.3. Active acid sites concentration by NH_3-TPD

The curves of ammonia TPD presented in Fig. 7 contain one broad peak of ammonia desorption with maximum within temperature range 207-233°C (Table 4). Only for the catalyst

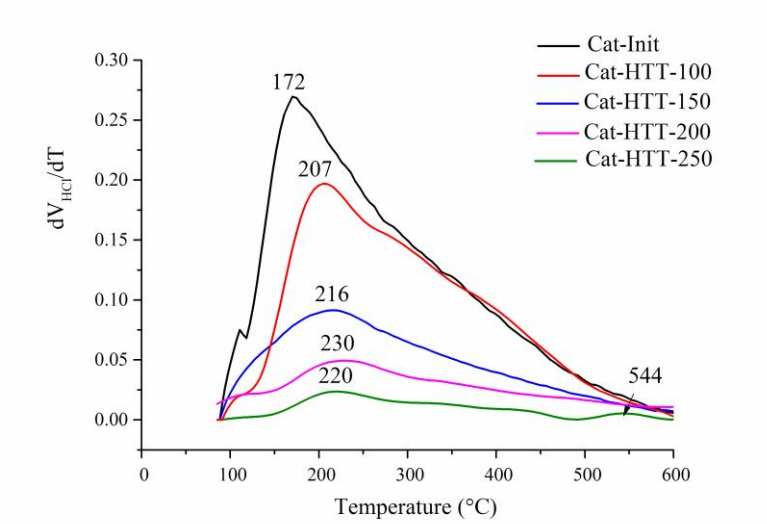

Fig. 7. NH_3-TPD curve for B–P–V–W–O_x catalyst supported on initial silica and silica hydrothermally treated at different temperature

This indicates the presence of predominantly weak and medium acid sites on the surface. This is consistent with results of other work devoted to investigation of boron oxide acidity [42]. However, asymmetry of peaks toward higher temperatures also evidences existence of more acidic groups on the surface. Thus, the second peak at about 544ºC is detected in the TPD curve for catalyst Cat-HTT-250 (Fig. 7). These sites can be attributed to phosphate-groups of BPO_4, acidity of which were studied using ammonia TPD [46,47]. So, it can be assumed that the surface groups B-OH and P-OH are weak and medium or strong acid sites, respectively.

The results calculated from TPD curves are presented in Table 4. The catalyst based on initial silica is an exception since maximum on ammonia TPD curve for this catalyst is detected at 172°C. This may be associated with the contribution of silanol groups, which were registered in FTIR spectra (Fig. 4) and are weakly acidic [24,46,48]. These groups can be accessible for ammonia molecules because the coverage of initial (untreated) silica with the active phase is still not continuous as mentioned above. The degree of surface coating with the deposited phase for other catalysts is higher, and therefore, the peak from SiOH-groups decreases.

The total acidity (in mmol/g) monotonically decreases with the support HTT temperature elevation (column 4). This is obviously associated with the same reduction in specific surface area (Table 1). The intensity of a.b. corresponding to surface hydroxyl groups in FTIR-spectra of supported catalysts decreases in the same sequence (Fig. 4).

Table 4**.** The acid sites concentration calculated from ammonia TPD curves

N	Sample	Temperature of peak (°C)	Total concentration of acid sites	
			(mmol/g)	(μmol/m^2)
1	2	3	4	5
1	Cat-Init	172	0.44	1.85
2	Cat-HTT-100	207	0.42	1.72
3	Cat-HTT-125	215	0.24	1.05
4	Cat-HTT-150	216	0.16	0.82
5	Cat-HTT-175	233	0.12	0.92
6	Cat-HTT-200	230	0.13	1.21
7	Cat-HTT-225	217	0.10	1.24
8	Cat-HTT-250	220	0.08	1.29

In contrast to total acid sites concentration per mass unit, the dependence of total acid sites concentration expressed in μmol/m^2 on HTT temperature of the support has a sharp minimum at 150°C (Table 4). Perhaps it is associated with a different thickness and structure of the layer of the deposited active phase in pores of different sizes (Table 2), different active phase distribution on surface of the support (Table 3) and, as a result, different acid-base properties (the ratio of acid and base sites) of the catalysts supported on silica hydrothermally treated at 100-250°C.

3.1.4. Active base sites concentration by acetic acid adsorption

The absolute isotherms of AcA adsorption (in μmol/m^2) obtained for initial silica and some supported catalysts are presented in Fig. 8. It should be noted that the initial parts of isotherms, corresponding to the formation of a monolayer and obeying the BET equation (p/p_0 value up to 0.25-0.28), are informative for characterizing the surface. It is well known that acetic acid, as well as other carboxylic acids, is adsorbed strongly, but physically, on silica -OH groups [24, 49 and references to these papers]. As can be seen in Fig. 8, the isotherm obtained for initial silica support is located below the others. Four isotherms obtained for catalysts, supported on initial silica and silica treated at different temperature, are located close to each other and partially superimposed. Finally, the isotherm for catalyst based on silica, hydrothermally treated at 150°C, is significantly higher than all the others. The excess of AcA adsorption value for the supported catalysts over that for the initial silica can be considered as a measure for basicity of deposited phase. Therefore, an interesting experimental fact is observed: the catalyst Cat-HTT-150 has the maximum ability of acetic acid sorption. On the other hand, this catalyst is also characterized by the minimum of acid sites concentration expressed in μmol/m^2 (Table 4). This may indicate bi-functional nature of studied supported catalysts. As a result, HTT of the support can be considered as a way for acid-base ratio regulation.

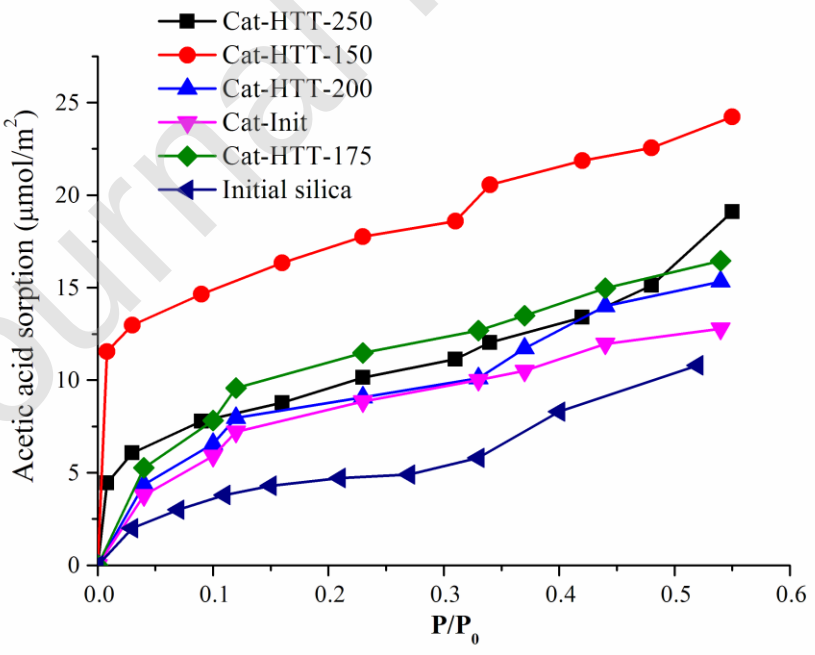

Fig. 8. Acetic acid sorption on initial silica and B–P–V–W–O_x catalyst supported on initial silica and silica treated by HTT at different temperature

3.2. Catalytic performance

3.2.1. Effect of support HTT temperature

Preliminary HTT of silica support has significant effect on catalytic properties of B–P–V–W–O_x/SiO_2 catalyst, namely reagents conversion and products selectivity. Elevation of support HTT temperature from 100 to 150°C results in increase of AcA conversion (*X*, %), while further elevation of HTT temperature leads to considerable decrease in conversion (Fig. 9a). Rise of reaction temperature naturally results in AcA conversion increase. The highest achieved value of AcA conversion is 81.2%. Such kind of dependence is connected with the porous structure of both supports and catalysts based on them. Firstly, although the specific surface area S_{N2} of catalysts based on supports treated at 100-150°C decreases, its accessibility for the molecules of reagents as well as the ability of the reaction products to leave the catalyst's surface increase (Fig. 10, Table 2). The latter is confirmed by some increase in S_{AcA} and decrease in excess of S_{N2} over S_{AcA} in indicated range of HTT. Besides, increase of predominant pore size from 9.7 to 12.6 nm takes place (inset to Fig. S2, Table 2). Therefore, possible diffusion resistance is eliminated.

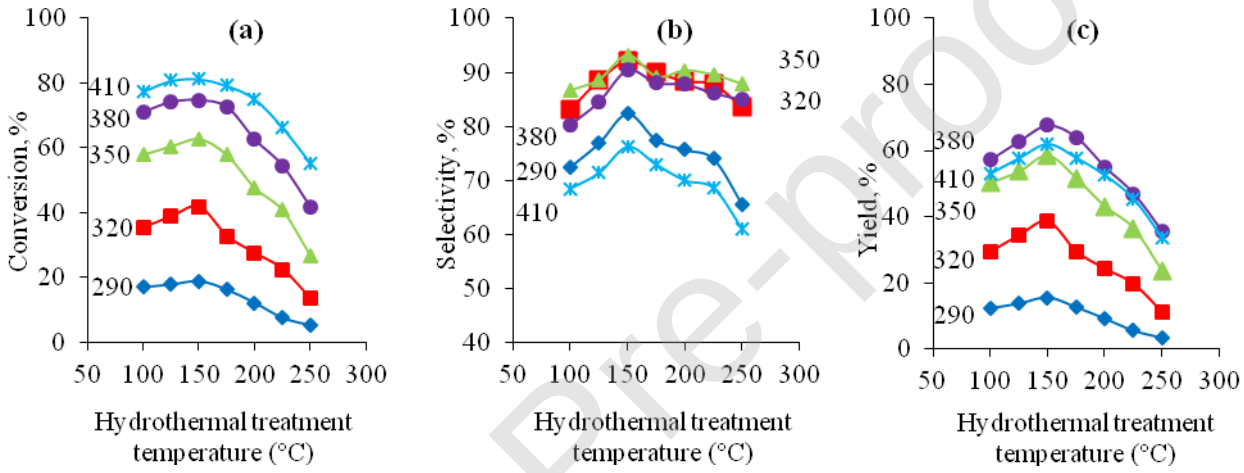

Fig. 9. The effect of the support HTT temperature on acetic acid conversion (a), acrylic acid selectivity (b) and acrylic acid yield (c) at different reaction temperatures (space time 8 s, the reactants molar ratio AcA:FA = 1:1)

Secondly, for catalysts based on supports treated at higher temperature (>150°C), the value of specific surface area has decisive importance: its reduction is accompanied by a decrease in conversion. As can be seen from Table 2, S_{N2} and S_{AcA} values are almost the same in this case. Obviously, the pore size of silica support about 10 – 13 nm is optimal for preparation of active supported catalyst.

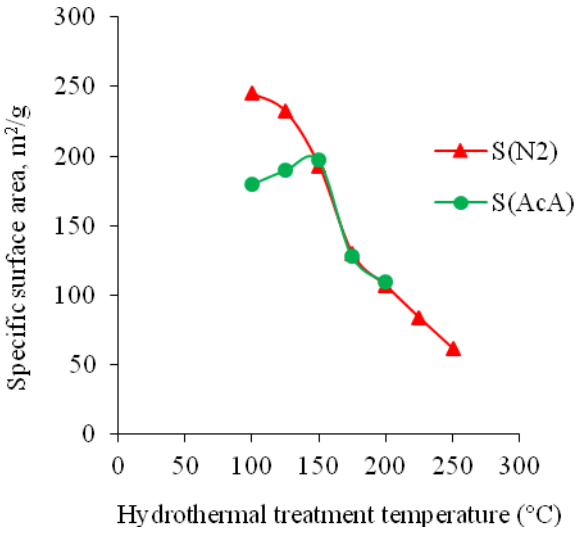

Fig. 10. The effect of the support HTT temperature on specific surface area S_{N2} and S_{AcA} of supported B–P–V–W–O_x/SiO_2 catalysts

Besides, increase of the reagents conversion using the Cat-HTT-150 additionally might be connected with increase of its basicity and ability to sorb acetic acid (Fig. 8) that is consistent with publication [13].

Selectivity of AA formation (*S*, %) also increases with elevation of HTT temperature of support up to 150°C and decreases with further elevation of HTT temperature. Maximal value of AA selectivity (93.1%) is achieved at reaction temperature equal to 350°C. However, some catalysts (after HTT of the support at 125, 150 and 175°C) allow to obtain almost the same result at 320°C (Fig. 10). So, the highest acrylic acid formation selectivity is achieved at reaction temperature 320–380°C on the catalysts based on silica gel treated hydrothermally at 125-175°C. It is known that usually selectivity for acid catalytic processes depends on the number and strength of surface acid sites [10, 11, 46, 47, 49]. Surprisingly, the maximum in dependence selectivity – temperature of support HTT (Fig. 9b) corresponds to minimum in the same dependence of total acidity expressed in μmol/m^2 (Table 4, column 5). Such behaviour is associated with better ability of acetic acid to sorption on surface of the catalysts, which are modified hydrothermally at about 150°C (Fig. 8), as well as with bi-functional nature of the catalysts as was mentioned above. It can also be noted that the presence of acid sites of low and medium strength (as was mentioned above) promotes the condensation processes that is consistent with the literature data [10-12, 49, 50]. Decrease of AA selectivity over the catalysts based on silica gel treated at higher temperatures (>150°C) is also associated with presence of strong acid sites on the catalysts surface. The latter is confirmed by slight shift of TPD-NH_3 curves toward higher temperatures when increasing the temperature of HTT, and by appearance of the second peak on the curves at high temperature – at 544°C (Fig. 7).

As a result, acrylic acid yield (*Y*, %) dependence on support HTT temperature also has a maximum at 150°C (Fig. 9c). Maximal yield (67.6 %) is achieved on this catalyst at reaction temperature 380°C.

3.2.2. Catalyst supported on hydrothermally treated silica vs catalyst supported on non-treated silica

To evaluate the expediency of catalyst support HTT in case of aldol condensation of AcA with FA, let us compare the efficiency of the catalyst supported on silica undergone HTT at the temperature found to be optimal (150°C) and the catalyst supported on initial silica gel.

The catalyst supported on silica after HTT allows to achieve higher AcA conversion compared to the catalyst supported on non-treated silica at reaction temperatures above 300°C (Fig. 11a).

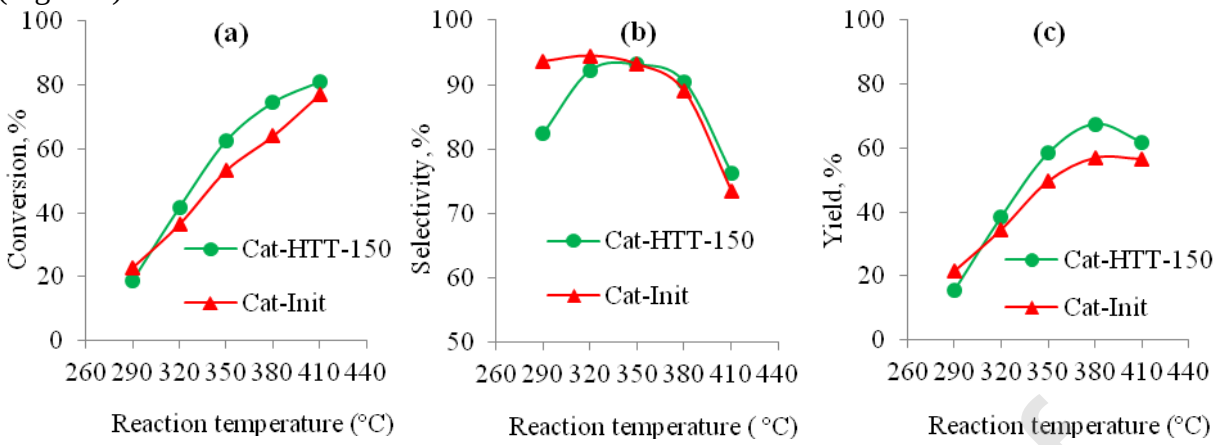

Fig. 11. Comparison of the catalysts Cat-Init and Cat-HTT-150 in the terms of acetic acid conversion (a), acrylic acid selectivity (b) and acrylic acid yield (c) at different reaction temperatures (space time 8 s, the reactants molar ratio AcA:FA = 1:1)

Hydrothermal treatment of the catalyst support has no substantial positive effect on acrylic acid selectivity (Fig. 11b). Slight increase of selectivity takes place at the reaction temperatures above 350°C and taking into account the fact that suitable acrylic acid yield is also achieved within this temperature range (350 – 410°C), generally HTT has positive effect on catalysts selectivity.

Acrylic acid yield increases with increasing the reaction temperature and reaches maximum at 380°C, afterward it starts decreasing (Fig. 11c). Maximum value of the yield achieved using the catalyst Cat-Init is 57.0 %. On the other hand, the yield achieved under the same conditions using the catalyst Cat-HTT-150 is 67.6%. So, the increase in acrylic acid yield due to the hydrothermal treatment of the catalyst support before the active phase deposition is 10.6 %, and this is achieved mainly because of increase in acetic acid conversion and slightly because of increase in acrylic acid selectivity.

The acetone formation as main side product at the reaction conditions was observed. Acetone selectivity fits within the range 3 - 18 % (in the presence of HTT 150 °C catalyst) and increases with elevation the reaction temperature. At optimum reaction conditions acetone selectivity was 6.5 %.

It must be admitted that support has crucial impact on the performance of B-P-V-W-O_x catalysts. Thus, unsupported catalyst of the same composition shows quite low catalytic performance and AA yield does not exceed 3.5 % based on acetic acid feed in. The difference is caused mainly due to the low specific surface area and lower surface concentration of active site as well as their accessibility for molecules of reagents. This emphasize the huge impact of porous structure of the catalysts for aldol condensation reactions, and the porous structure can be easily adjusted in wide limits via support modification.

4. Conclusions

B–P–V–W oxide catalyst supported on mesoporous silica gel is efficient in gas-phase aldol condensation of acetic acid with formaldehyde to acrylic acid. Hydrothermal treatment of the silica support before deposition of the active phase even at constant qualitative and quantitative composition of the catalyst changes its physical and chemical properties in wide range resulting in its catalytic performance improvement. Preliminary hydrothermal treatment of the silica support within the temperature range 100 – 150 °C increases specific surface area (available for the reagents) of the catalyst, pore diameter and decreases the number of acid sites per mass unit

of the catalyst, change of strong/weak acid sites ratio, as well as ability to acetic acid sorption and basicity of the catalysts.

The optimal temperature of the hydrothermal treatment of the support in case of its duration 3 h is 150°C. The optimal temperature to carry out the condensation reaction at contact time 8 s is 380°C. Acrylic acid yield achieved under these conditions was 67.6% at 90.5% selectivity. The catalyst supported on the silica treated under optimal temperature 150°C allows to achieve acrylic acid yield about 10% higher compared to that achieved with the same catalyst supported on non-treated initial silica.

Thus, hydrothermal treatment of the catalyst support at certain temperature has positive effect on the catalyst performance and increases both acetic acid conversion and acrylic acid selectivity. These catalysts possess thermostability in the temperature range of catalysts operation (up to 410 °C). The hydrothermal treatment of support prevents coking of the catalyst which is promising in terms of catalyst life. The hydrothermal treatment of support can be suggested as a cheap and efficient way to modify the supported catalysts structure and their catalytic performance.

Based on high catalytic performance, it can be concluded that the developed catalysts are quite promising for industrial application. However, the conversion of initial reagents can be further improved, the data, shown in the work, were achieved at equimolar acetic acid/formaldehyde ratio (as opposed to most known results where an excess of acetic acid (3 – 5) is used). So the use of the B–P–V–W–O_x catalyst will potentially reduce energy consumption for recycling procedure.

Competing interest.

The authors declare no competing interest.

References

[1] M. Tanimoto, D. Nakamura, T. Kawajiri, Method for production of acrolein and acrylic acid from propylene. Patent 6545178 US, 2003.

[2] Acrylates – Advances in Research and Application Science. Ed. Q.A.Acton, 2013 pp.779.

[3] R. Nebesnyi, East. Europ. J. Enterprise Technol. 1 (2015) 13-16.

[4] L. Liu, X.P. Ye, J.J. Bozell, Chem. Sus. Chem. 5 (2012**)** 1162-1180.

[5] L. Rong, W. Tiefeng, C. Dali, J. Yong, Ind. Eng. Chem. Res. 53 (2014) 8667-8674.

[6] C. Gao, C. Ma, P. Xu, Biotechnol. Adv. 29 (2011**)** 930-939.

[7] M. Goebel, C. Walsdorff, M. Hartmann, N.T. Wörz, T. Blaschke, P. Grüne, Process for preparing acrylic acid with high space-time yield. Patent EP2997004A1, BASF SE, 2016.

[8] M. Ai, J. Catal. 107 (1987) 201-208.

[9] M. Ai, Appl. Catal. 54 (1989**)** 29-36.

[10] M. Ai, H. Fujihashi, S. Hosoi, A. Yoshida, Appl. Catal. A: Gen. 252 (2003) 185-191.

[11] D. Yang, D. Li, H. Yao, G. Zhang, T. Jiao, Z. Li, C. Li, S. Zhang, Ind. Eng. Chem. Res. 54 (2015) 6865-6873.

[12] D. Yang, C. Sararuk, K. Suzuki, Z. Li, C. Li, Chem. Eng. J. 300 (2016) 160-168.

[13] J. Hu, Z. Lu, H. Yin, W. Xue, A. Wang, L. Shen, S. Liu, J. Ind. Eng. Chem. 40 (2016**)** 145-151.

[14] A. Wang, J. Hu, H. Yin, Z. Lu, W. Xue, L. Shen, S. Liu, RSC Adv. 7 (2017) 48475-48485.

[15] Y. Nebesna, V. Ivasiv, R. Nebesnyi, East. Europ. J. Enterprise Technol. 6 (2015) 49–52.

[16] Y. Dmytruk, V. Ivasiv, R. Nebesnyi, S. Maykova, East. Europ. J. Enterprise Technol. 4 (2015) 4-7.

[17] R. Nebesnyi, V. Ivasiv, Z. Pikh, V. Zhyznevskyi, Y. Dmytruk, Y. Chem. Chem. Technol. Lviv. 8 (2014) 29-34.

[18] N. Lapychak, V. Ivasiv, R. Nebesnyi, Z. Pikh, I. Shpyrka, East. Europ. J. Enterprise Technol. 83 (2016) 44 – 48.

[19] J. Skubiszewska-Zieba, S. Khalameida, V. Sydorchuk, Colloids Surf. A: Physicochem. Eng. Aspects, 504 (2016**)** 139-153.

[20] R. Leboda, B. Charmas, V. Sidorchuk, Adsorp. Sci. Technol. 15 (1997) 189-214.

[21] C.J. Brinker, G.W. Scherer, Sol-Gel Science: The Physics and Chemistry of Sol-Gel Processing: Academic Press: San Diego, CA, 1990 pp.633.

[22] R. Leboda, V. Tertykh, V. Sidorchuk, J. Skubiszewska-Zięba, Colloids Surf. A: 135 (1998**)** 253–265.

[23] R. Leboda, E. Mendyk, V. Tertykh, Matter Chem. Phys. 42 (1995) 7–11.

[24] R.K. Iler, The Chemistry of Silica, Solubility, Polymerization, Colloid and Surface Properties, and Biochemistry: John Wiley & Sons: New York, 1979.

[25] L. Zhuravlev, Colloids Surf. A: 173 (2000**)** 1–38.

[26] A. Christy, Ind. Eng. Chem. Res. 50 (2011) 5543–5549.

[27] R. Leboda, B. Charmas, V. Sidorchuk, Adsorp. Sci. Technol. 15 (1997) 215-230.

[28] D. Maidannik, V. Sidorchuk, V. Tertykh, Russ. J. Appl. Chem. 64 (1991**)** 1867-1870 (in russ).

[29] V. Sidorchuk, R. Leboda, D. Maydannik, V. Tertykh, J. Colloid Interface Sci. 171 (1995) 168 - 172.

[30] G. Leofanti, M. Padovan, G. Tozzola, B. Venturelli, Catal. Today 41 (1998) 207-219.

[31] Y. Zeng, C. Fan, D. Do, D. Nicholson, Ind. Eng. Chem. Res. 53 (2014) 15467–15474.

[32] S. Khalameida, V. Sydorchuk, J. Skubiszewska-Zięba, B. Charmas, E. Skwarek, W. Janusz, J. Therm. Anal. Calorim. 128 (2017) 795–806.

[33] S. Khalameida, V. Diyuk, A. Zaderko, V. Sydorchuk, J. Skubiszewska-Zięba, J. Therm. Anal. Calorim. 131 (2018) 2361-2371.

[34] R. Ahmed, C. Sinnathambi, D. Subbarao, J. Appl. Sci. 11 (2011) 1225-1230.

[35] S. Khalameida, R. Nebesnyi, Z. Pikh, V. Ivasiv, V. Sydorchuk, Y. Nebesna, I. Shpyrka, B. Charmas, K. Kucio, Reac. Kinet. Mech. Cat. 125 (2018) 807- 825.

[36] F. He, Z. He, J. Xie, Yu. Li, Amer. J. Analytic. Chem. 5 (2014) 1142-1150.

[37] N. Okazaki, M. Takahashi, H. Murai, A. Tada, Phosphorus Res. Bull. 9 (1999) 63-68.

[38] R. Wang, H.Jiang, H.Gong, J.Zhang, Mater. Res. Bull. 47 (2012) 2108–2111.

[39] C. Zhang, C. Lin, C. Li, Z. Quan, X. Liu, J. Lin, J. Phys. Chem. C 112 (2008) 2183-2192

[40] S. Chen, M.Ye, H.Chen, X.Yang, J.Zhao, J. Inorg. Organomet. Polym. 19 (2009) 139–142.

[41] P. Kmecl, P. Bukovec, Acta Chim. Slov. 46 (1999) 161-171.

[42] S. Imamura, K. Imakubo, S. Furuyoshi, Ind. Eng. Chem. Res. 30 (1991) 2355-2358.

[43] A. Pilli, J. Jones, V. Lee, N. Chugh, J. Kelber, F. Pasquale, A. LaVoie, J. Vac. Sci. Technol A: 36 (2018) 061503 doi:10.1116/1.5044396

[44] C.D. Wagner, W.M. Riggs, L.E. Davis, J.F. Moulder, G.E. Muilenberg (Eds.), Handbook of X-ray Photoelectron Spectroscopy, Perkin-Elmer Corp., Phys. Elect. Div., Minesota, 1979.

[45] V.V. Atuchin, I.B. Troitskaia, O.Y. Khyzhun, V.L. Bekenev, Y. M. Solonin, Appl. Mechanics Mater. 110-116 (2012) 2188-2193.

[46] Yu. Li, Y. Wang, X. Yang, X.Liu, Y. Yang, J. Hao, J. Therm. Anal. Calorim. 129 (2017) 1491-1494.

[47] P. Bhaumik, T. Kane, P. Dhepe, Catal. Sci. Technol. 4 (2014) 2904-2907.

[48] V. Sidorchuk, V. Tertykh, R. Leboda, B. Charmas, Adsorp. Sci. Technol. 14 (1996) 339-347.

[49] D. Mao, G. Lu, Q. Chen, Z. Xie, Yu. Zhang, Catal. Lett. 77 (2001) 119-124.

[50] X. Feng, Bo. Sun, Y. Yao, Q. Su, Ji W. Weijie, Ch.T.Au, J. Catal. 314 (2014) 132–141.